



**HAL**  
open science

## New Visual Analytics Tool and Spatial Statistics to Explore Archeological Data: The Case of the Paleolithic Sequence of La Roche-à-Pierrot, Saint-Césaire, France

Armelle Couillet, Hélène Rougier, Dominique Todisco, Josserand Marot,  
Olivier Gillet, Isabelle Crevecoeur

### ► To cite this version:

Armelle Couillet, Hélène Rougier, Dominique Todisco, Josserand Marot, Olivier Gillet, et al.. New Visual Analytics Tool and Spatial Statistics to Explore Archeological Data: The Case of the Paleolithic Sequence of La Roche-à-Pierrot, Saint-Césaire, France. *Journal of Computer Applications in Archaeology*, 2022, 5 (1), pp.19 - 34. 10.5334/jcaa.81 . halshs-03596369

**HAL Id: halshs-03596369**

<https://shs.hal.science/halshs-03596369v1>

Submitted on 14 Feb 2024

**HAL** is a multi-disciplinary open access archive for the deposit and dissemination of scientific research documents, whether they are published or not. The documents may come from teaching and research institutions in France or abroad, or from public or private research centers.

L'archive ouverte pluridisciplinaire **HAL**, est destinée au dépôt et à la diffusion de documents scientifiques de niveau recherche, publiés ou non, émanant des établissements d'enseignement et de recherche français ou étrangers, des laboratoires publics ou privés.



Distributed under a Creative Commons Attribution 4.0 International License

# New Visual Analytics Tool and Spatial Statistics to Explore Archeological Data: The Case of the Paleolithic Sequence of La Roche-à-Pierrot, Saint-Césaire, France



## RESEARCH ARTICLE

]u[ubiquity press

ARMELLE COUILLET

HÉLÈNE ROUGIER

DOMINIQUE TODISCO

JOSSERAND MAROT

OLIVIER GILLET

ISABELLE CREVECOEUR

*\*Author affiliations can be found in the back matter of this article*

## ABSTRACT

The archeological record of La Roche-à-Pierrot (France) is central to debates on the Middle to Upper Paleolithic transition. To this day, it is the only site to have provided a relatively complete Neandertal skeleton associated with an industry identified as transitional, the Châtelperronian, which had been attributed until then to *Homo sapiens*. The site was the subject of several excavation campaigns led by F. Lévêque in the 1970s, 1980s, and 1990s, and ongoing fieldwork resumed in 2013. Spatial representations and statistical analyses of the original excavation data are of invaluable help in assessing the coherence of the first archeological stratigraphy established in the 1970s. A 3D reconstruction of Lévêque's spit record was developed for exploratory purposes, based on reassessment of the faunal collection and completed by information recorded in the excavation notebooks filled out by Lévêque's team. It was then used in order to evaluate the feasibility of modeling the data recorded during the first excavations. Geovisualization tools, associated with appropriate 3D spatial statistics using the Queen contiguity applied to the archeological sequence, such as the similarity and coherence indices, provided an understanding of the spatial inconsistencies in the first archeological sequence, as well as revealed the spatial organization (geometry) of the archeostratigraphic units. The resulting interactive visualization application provides researchers with a new tool to explore the stratigraphic units spatially, as well as according to their indices. Where inconsistencies are observed, use of similarity and coherence indices allows discussion of any biases potentially related to topography, spatial heterogeneity of the deposits (facies), excavation history, or primary data acquisition/recording. Such spatial analyses contribute to a better understanding of site formation processes and provide novel means to explore archival information interactively, as well as to produce models including data from old and new excavations on the same site.

## CORRESPONDING AUTHOR:

**Armelle Couillet**

Rouen Normandie University,  
CNRS UMR 6266 IDEES, 76130  
Rouen, FR

[armelle.couillet@cnrs.fr](mailto:armelle.couillet@cnrs.fr)

## KEYWORDS:

3D geovisualization; spatial statistics; digital archeology; archeological archives; archeostratigraphy

## TO CITE THIS ARTICLE:

Couillet, A, Rougier, H, Todisco, D, Marot, J, Gillet, O and Crevecoeur, I. 2022. New Visual Analytics Tool and Spatial Statistics to Explore Archeological Data: The Case of the Paleolithic Sequence of La Roche-à-Pierrot, Saint-Césaire, France. *Journal of Computer Applications in Archaeology*, 5(1), 19–34. DOI: <https://doi.org/10.5334/jcaa.81>

## 1 INTRODUCTION

The site of La Roche-à-Pierrot in Saint-Césaire (France) is central to one of the most keenly-debated topics in paleoanthropology and Paleolithic archeology: the disappearance of Neandertals and their replacement by *Homo sapiens* in Eurasia during the Middle-to-Upper Paleolithic transition period (e.g. Zilhão and d'Errico 1999; Mellars 2004; Talamo et al. 2020). It is known for having yielded an exceptional sequence of Mousterian, Châtelperronian and Aurignacian occupations (Lévêque et al. 1993), and is also the only site known to have produced a rather complete Neandertal skeleton (Saint-Césaire 1) within a Châtelperronian context (Lévêque & Vandermeersch 1980, 1981). However, this Neandertal/Châtelperronian association has been called into question through the years (e.g. Bar-Yosef & Bordes 2010), and a reassessment of the lithic assemblage from the so-called Châtelperronian level (EJOP sup), including its distribution and taphonomy, has recently exposed the lack of reliable evidence for it (Gravina et al. 2018). New excavations began at Saint-Césaire in 2013 with the aim of identifying the site formation processes from a geoarcheological perspective (Bachelierie et al. 2014). This on-going project was extended in 2015 to include the new data from the field in the reassessment of all of the data from the original excavations, including archival information, using both classical and state-of-the-art modeling and analytical methods (Crevecoeur 2017).

Because archeological phenomena have an intrinsic spatial component, the tools used to study geospatial data and information play a key role (Hodder & Orton 1976), such as in the understanding of activity patterns and human behavior in space (Hietala 1984). In this context, new digital tools such as Geographic Information Systems (GIS), 3D geovisualization and photogrammetry hold a prominent place, given their increasing utility and ability to extract, study, and characterize the spatial dimension of archeological data (e.g. 3D models), especially on an intra-site scale (Discamps et al. 2016; Dilella & Soressi 2020). Such tools can be applied to archival documentation (e.g. photographs, maps, drawings) and stratigraphic excavation sequences, and are particularly useful to complement the use of classical spatial statistics or spatial taphonomy for interpreting Pleistocene palimpsests and thereby test site integrity (Discamps et al. 2019). In this way, digital archeology and GIS allow complex spatial statistical analyses to be performed based on 2D or 3D data for a better understanding of site formation processes, whether anthropogenic or natural.

One way to study archeological sequences and deposit geometry relies on digital visualization systems to facilitate the creation, presentation, and exploration of stratigraphic relationships (Galeazzi et al. 2016). Insofar as stratigraphic sequences are generally viewed as static (two-dimensional, diagrammatic representations that

are difficult to manipulate or correlate spatially), 3D geometrical rendering techniques applied to intra-site data recordings are particularly useful (Galeazzi 2015). Applying a holistic approach, they provide an effective way to use archives and the possibility of linking archival datasets to a dynamic and realistic 3D reproduction of the excavations, thereby enhancing understanding of the spatial relationships between units, layers, eco- and artefacts of stratigraphic sequences. In addition to providing a user-friendly and effective means of navigating stratigraphic and associated data, and testing the relative chronology of deposits, geovisualization can also help to adjust excavation strategies.

The present work proposes a new visual analytics tool and spatial statistics to explore archival archeological data. In the context of the La Roche-à-Pierrot excavations, selection of a georeferenced 3D web-based representation followed the rationale put forward by Galeazzi et al. (2016) in terms of effective collaboration and archive interpretation enhancement. By anchoring this work within the framework of reflexive methods of analysis (Lercari 2017) and the sense-making loop for visual analytics (Van Wijk 2005; Opgenhaffen 2021), the spatial analysis method typically used for 2D data was integrated into the 3D modeling in order to test inconsistencies in the archeostratigraphic information recorded during the original excavations at La Roche-à-Pierrot (Lévêque & Vandermeersch 1980, 1981; Lévêque et al. 1993) based on two new indices we computed: the similarity index (SI) and the coherence index (CI).

## 2 MATERIALS AND METHODS

### 2.1 MATERIALS

The archeological site of La Roche-à-Pierrot is located in the town of Saint-Césaire, about ten kilometers east of the city of Saintes in Charente-Maritime, Southwestern France. It is located around 35 meters a.s.l., and 2–4 meters above the current floodplain of the Coran River (*Figure 1*). The original excavations were directed by François Lévêque and lasted from 1977 to 1987, with an additional field season in 1993 (Lévêque et al. 1993; Backer 1994). Anna Backer directed a final field season in 1997 with the aim of cleaning the site, recording its state of preservation, and providing recommendations for its future conservation (Backer 1997). The archeostratigraphy from Lévêque's excavations at the base of an Upper Turonian limestone cliff is divided into two principal sets: the upper, yellow sequence (*ensemble jaune* or EJ) and the lower, gray sequence (*ensemble gris* or EG) (Miskovsky & Lévêque 1993). Each sequence is further divided into several levels based on sedimentologic and colorimetric criteria that are reflected in the names of the layers (e.g. EJO = *ensemble jaune-orange*; *Figure 2*).

The excavations at Saint-Césaire used a one-square-meter grid system and proceeded by 50 × 50 cm<sup>2</sup> sub-

squares and 5 or 10 cm spits (Lévêque 2002) (Figure 1). An excavation notebook was filled for each square with each excavator recording their name, the date, sub-square, spit and layer they were excavating, along with information pertaining to the piece-plotted objects (Figure 3). Relevant stratigraphical observations were sometimes added and could include diagrams. Sediments were sieved and sorted, and non-piece plotted lithic and faunal elements were bagged separately, each with a label indicating their excavation date and stratigraphical provenience (Figure 3).

The starting point of the present project was the encoding in a spreadsheet of the provenience of all of the non-piece plotted fauna from the original excavations. In a second stage, we compared this information with that of the excavation notebooks, in order to confirm the congruence between the information noted on the fauna bag labels and the field observations written in the

notebooks (Figure 4). This also allowed us to supplement the data from the non-piece plotted fauna with excavated spits from which no fauna had been recovered.

Where two or more levels were identified in a single spit, only the uppermost level according to Lévêque’s archeostratigraphy (Figure 2) was noted as present. This simplification method follows the stratigraphical logic and minimizes anomalies in order to make observations interpretable. This approach resulted in 10 different levels being recorded from the upper *ensemble jaune* (from top to bottom, EJJ, EJM, EJF, EJO, EJO sup, EJO inf, EJOP, EJOP sup, and EJOP inf, along with an undifferentiated EJ level) and six from the lower *ensemble gris* (EGPF, EGPS, EGP, EGF, EGC, and EGB).

Thanks to the detailed recording methods adopted by F. Lévêque at Saint-Césaire, we finally produced 4729 spreadsheet entries, each corresponding to a 50 × 50 × 5 cm spit. This covers a surface area of 205 sub-squares

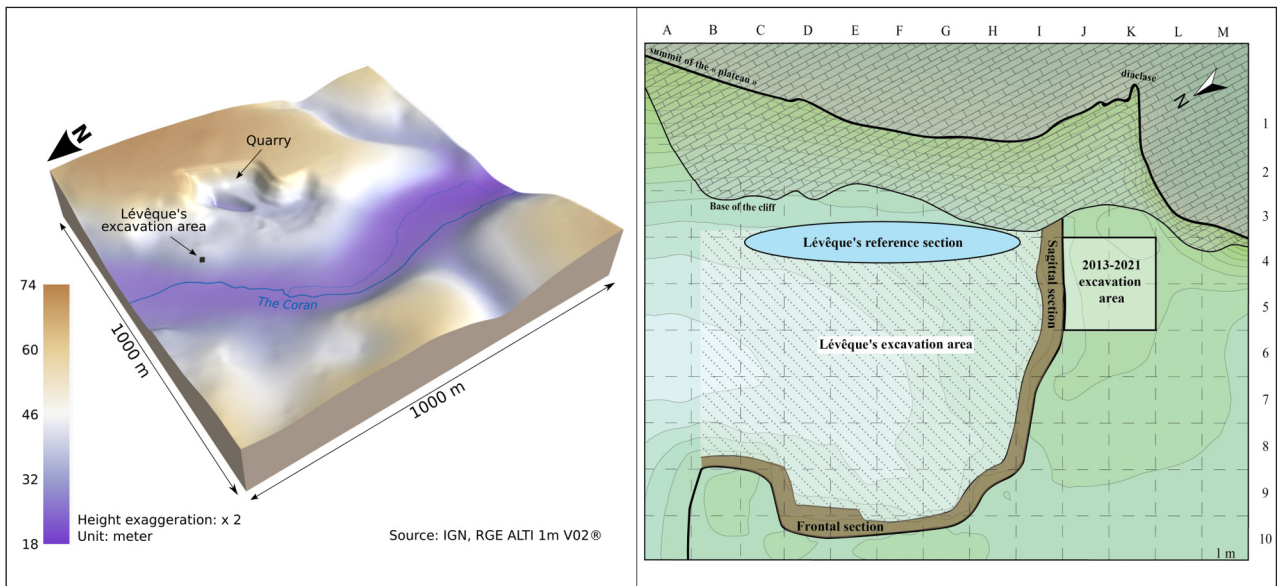


**Figure 1** Digital terrain model (left) and topographic map (right) of the La Roche-à-Pierrot archeological site with the location of the excavation grid and reference section of Lévêque’s excavation area, as well as the position of current fieldwork. Note the location of the reference section at the base of an Upper Turonian limestone cliff.

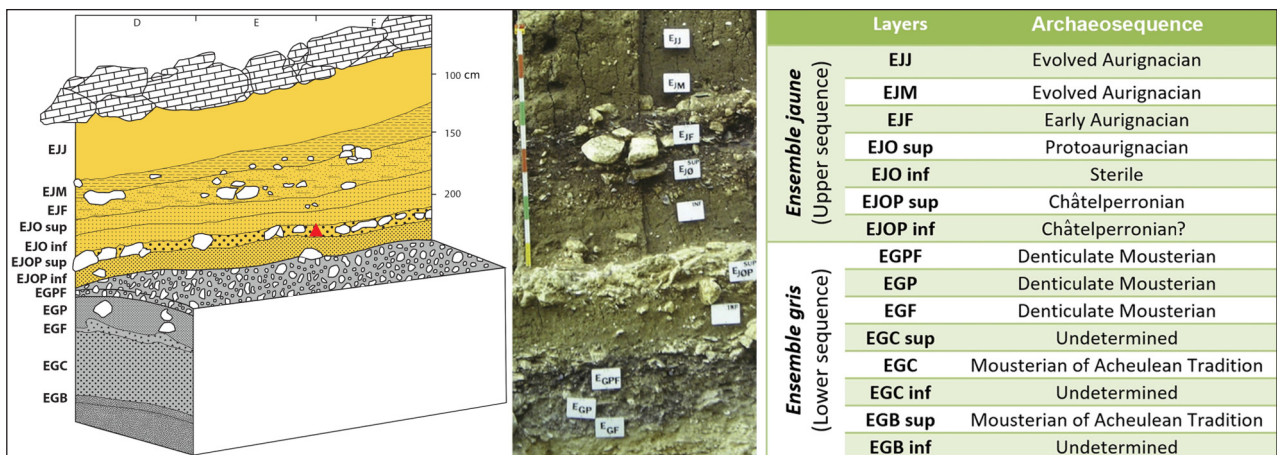


**Figure 2** Reference section (left) and sequence (right) of the archeological stratigraphy of La Roche-à-Pierrot (after Lévêque 1997). The red triangle indicates the location of the Saint-Césaire 1 Neandertal remains.

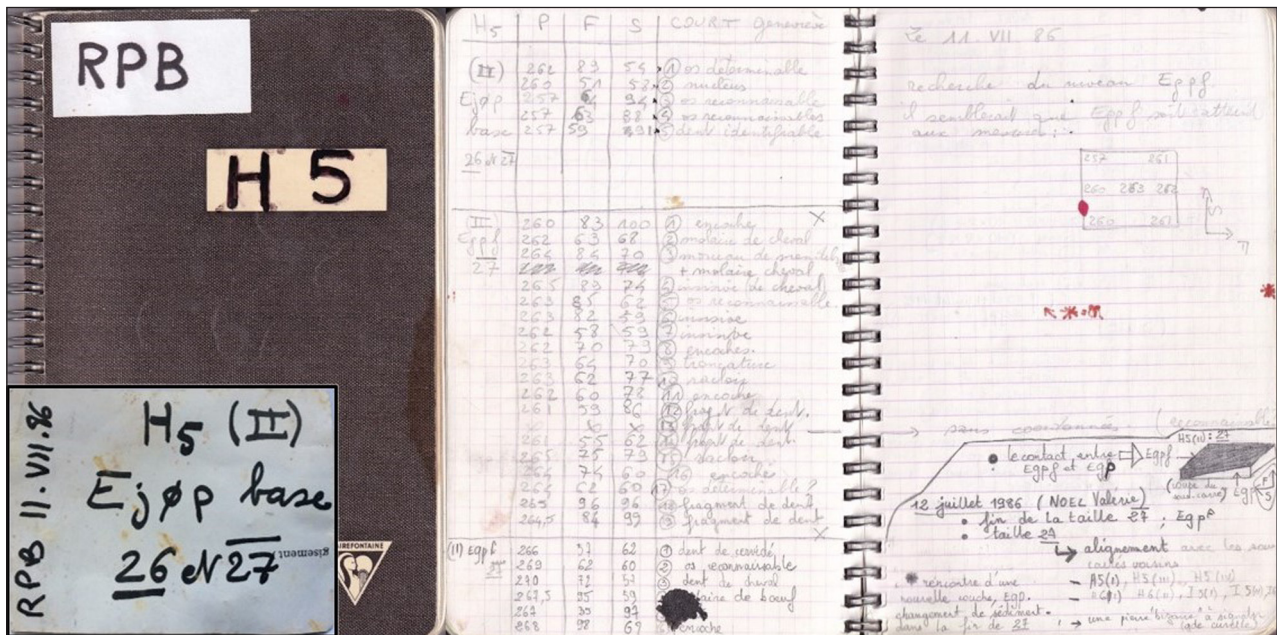


Figure 3 Example of the cover and contents of the excavation notebooks filled out during Lévêque’s fieldwork (square H5) and example of the labels associated with the bags of non-piece plotted faunal remains (inset).

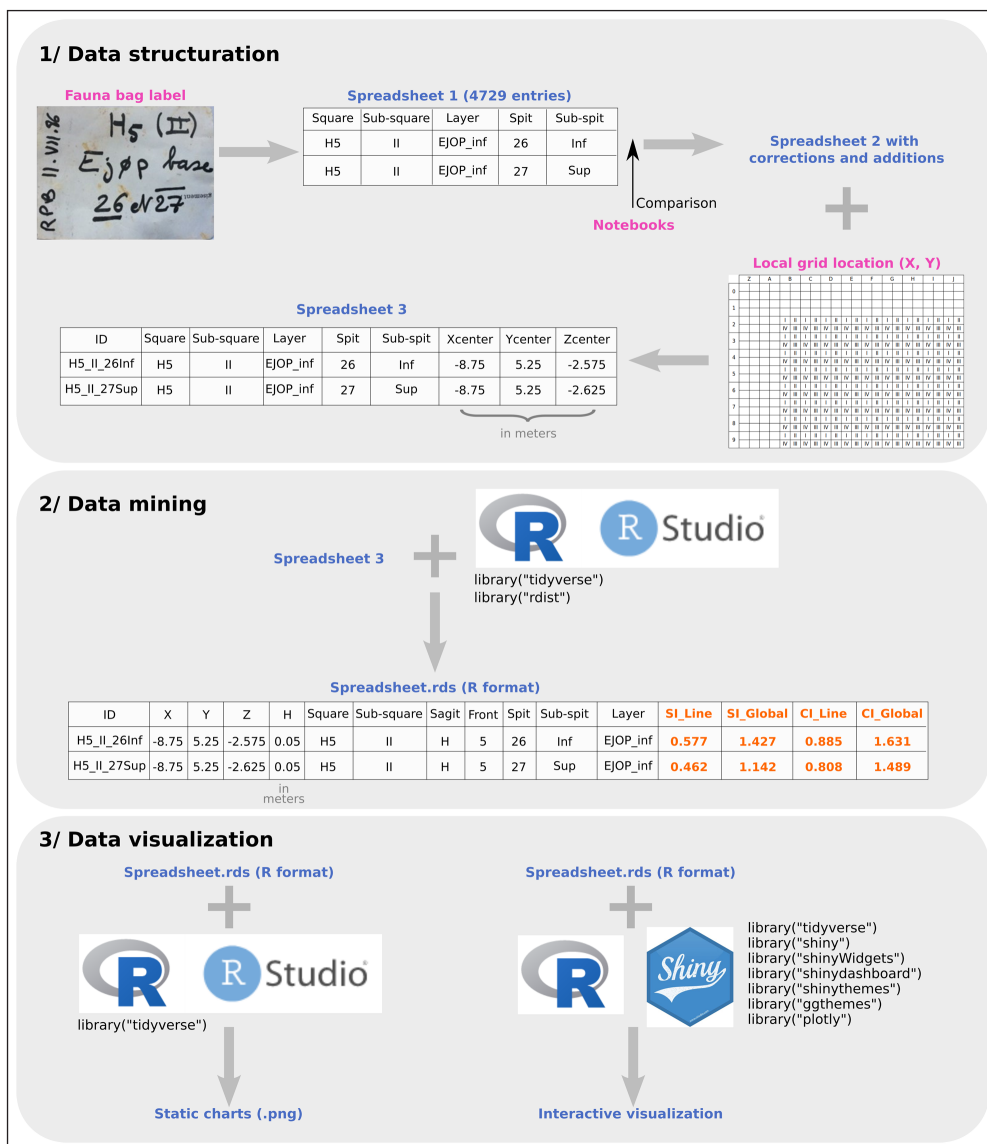


Figure 4 Process flowchart from data to interactive visualization.

(51.25 m<sup>2</sup>) and a total thickness per sub-square varying from 5 cm (in C3 III and I3 II, close to the cliff) to 2.25 m (in D5 III, E5 III, and E5 IV), for an estimated total volume of 62.55 m<sup>3</sup> of excavated sediments.

### 2.2 3D VISUALIZATION OF THE ARCHEOSEQUENCE

The first 3D visualization of the archeological stratigraphy of Saint-Césaire was produced using the Qgis2threejs plugin (Minoru 2013) (Figure 5). Spits were initially represented as polyhedra matching the three-dimensional scale. We then opted for cylindrical or cuboid shapes of smaller size (for x and y dimensions) in order to facilitate viewing inside the archeostratigraphy (Brath 2014; Kraus et al. 2021).

To produce effective visualizations and identify each of the 16 stratigraphic levels clearly, color ranges were chosen following the rules of graphic semiology (Bertin 1967) combining color variation and value variation (Figure 6). The limits of human eye perception (six to seven value levels including black and white) were taken into account in

selecting colors associated with variations in grey darkness (their value), in addition to ensuring that the different levels of the two yellow and grey principal stratigraphic units were readily distinguishable by combining the use of the three primary colors (yellow, cyan blue, and magenta). The 10 levels of the *ensemble jaune* were represented by colors based on high proportions of yellow, whereas those of the *ensemble gris* were represented by colors other than yellow and primarily based on blue.

### 2.3 3D COMPUTATION OF INDICES FOR BETTER DETECTION OF STRATIGRAPHIC INCONSISTENCIES AND CROSS-LAYER TRANSITIONS

Spatial analysis can provide tools for a better understanding of where inconsistencies are located and we proposed to adapt local measurements of spatial association (Anselin 2020) to stratigraphy, i.e. to a 3D structure. We analyzed the structure of the archeosequence by building a neighborhood matrix using the Queen contiguity: when considering all of the spits

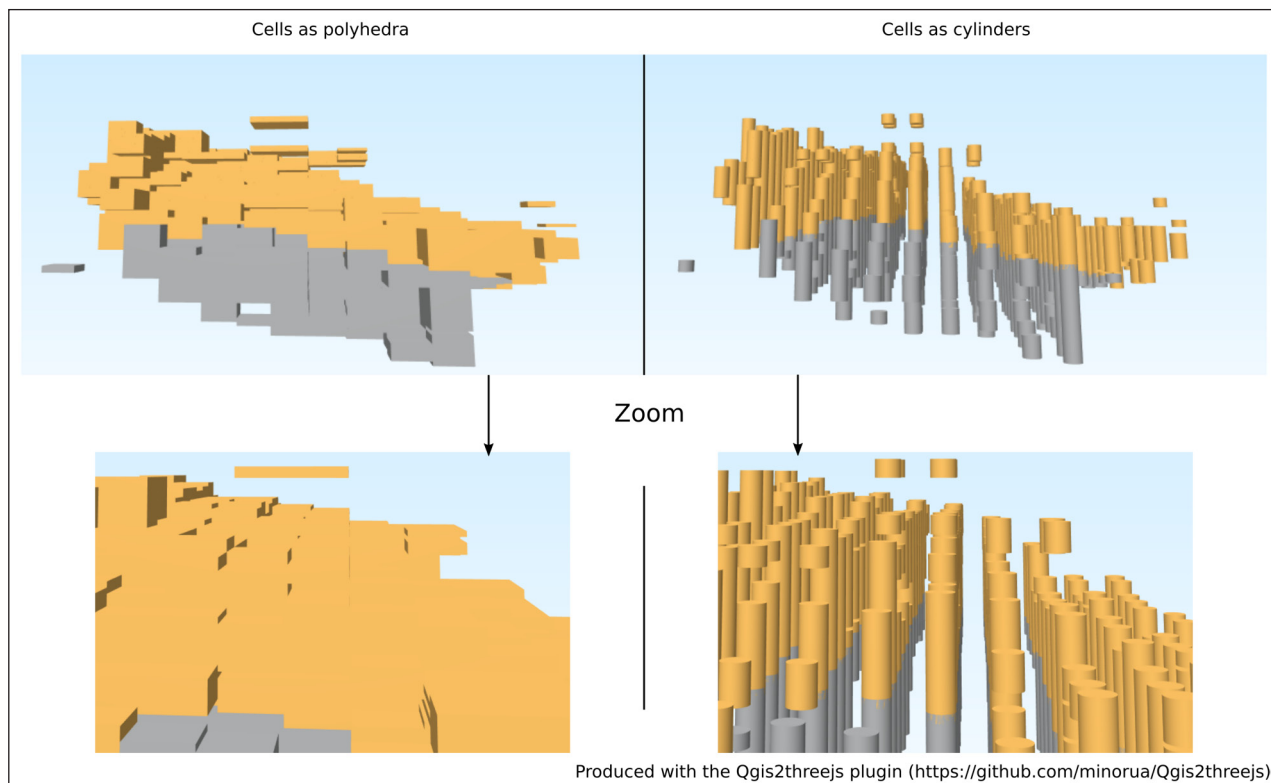


Figure 5 3D structure representation of the yellow and gray principal stratigraphic sequences of La Roche-à-Pierrot.

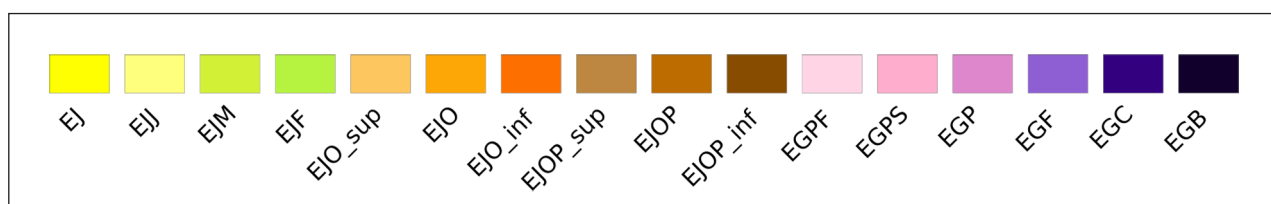


Figure 6 Color scheme selected for the levels of Lévêque's archeological stratigraphy, see Figure 2. EJ is a grouping of undifferentiated layers from the *ensemble jaune* and EGPS is a facies of EGP.

surrounding a given spit, we attributed a value of 1 to each neighbor if they corresponded to the fixed condition and of 0 if they did not. The maximum number of cells used to calculate the index was 26. Two spatial weight matrices were produced (Tiefelsdorf 1998; Anselin 2020) (*Figure 7*):

- A matrix with line standardization: for a given spit, the weight given to each of its neighbors was divided by the sum of the weights of its neighbors. While easy to interpret, this standardization method implies competition between neighbors, since the fewer neighbors a spit has, the more weight each carries. Indices computed using this standardization method vary between 0 and 1.
- A matrix with global standardization: the sum of all of the weights equals the number of spits. This standardization method averts edge effects since the calculation is not only based on the direct neighbors of each spit (whose number can vary from 0 to 26) but it also takes the whole of the entities into account.

Based on the 3D matrices computed in an R script (Bivand, Pebesma & Gómez-Rubio 2008), two indices were produced (*Figure 8*). The coherence index (CI) is at its maximum when all of the surrounding spits contain the same level as that of the considered spit OR when the levels of the spits located directly above and below the considered spit match the archeological sequence identified by F. Lévêque.

The value of the coherence index provides insight into the alignment of the location of each spit with the stratigraphic level assigned to it. The similarity index (SI) takes into account only the first condition of the CI and informs on the homogeneity of the stratigraphic levels.

### 3 RESULTS

#### 3.1 INTERACTIVE VISUALIZATION APPLICATION

The main purpose of the present application is to give the researchers on the La Roche-à-Pierrot Collective Research Project greater autonomy to explore the site deposits within the three geographic dimensions and across the index values as calculated above. For example, this approach may provide information that could supplement field observations and/or collection-based assumptions of potential reworking. To this end, the interactive application was duplicated: one for indices calculated with line standardization ([https://analytics.huma-num.fr/Armelle.Couillet/Archeo\\_2021B\\_lineSD/](https://analytics.huma-num.fr/Armelle.Couillet/Archeo_2021B_lineSD/)) and one with global standardization ([https://analytics.huma-num.fr/Armelle.Couillet/Archeo\\_2021B\\_globalSD/](https://analytics.huma-num.fr/Armelle.Couillet/Archeo_2021B_globalSD/)), with each of them containing three windows. The first window provides a basic 3D visualization of the levels of the site and a distribution chart of the levels (archeological sequence) (*Figure 9*).

Windows 2 and 3 are designed to a similar model: they provide 3D visualizations of the considered index (SI in window 2 and CI in window 3) with available interactive selection of different dimension values (i.e. according to depth, sagittal and frontal bands of the grid system) on one hand (*Figure 10*) and of the index value range on the other hand (*Figure 11*). Each 3D visualization is associated with an interactive graph resulting from the selected parameters or index value.

This 3D visualization model and associated indices make it possible to highlight quickly the areas of the site with particular patterns. *Figure 12* illustrates this analytical opportunity through the 3D representation of the coherence indices. From general site data, it is possible to extract certain areas of interest by selecting the desired depth and grid area. The index histograms are recalculated automatically on the selected area.

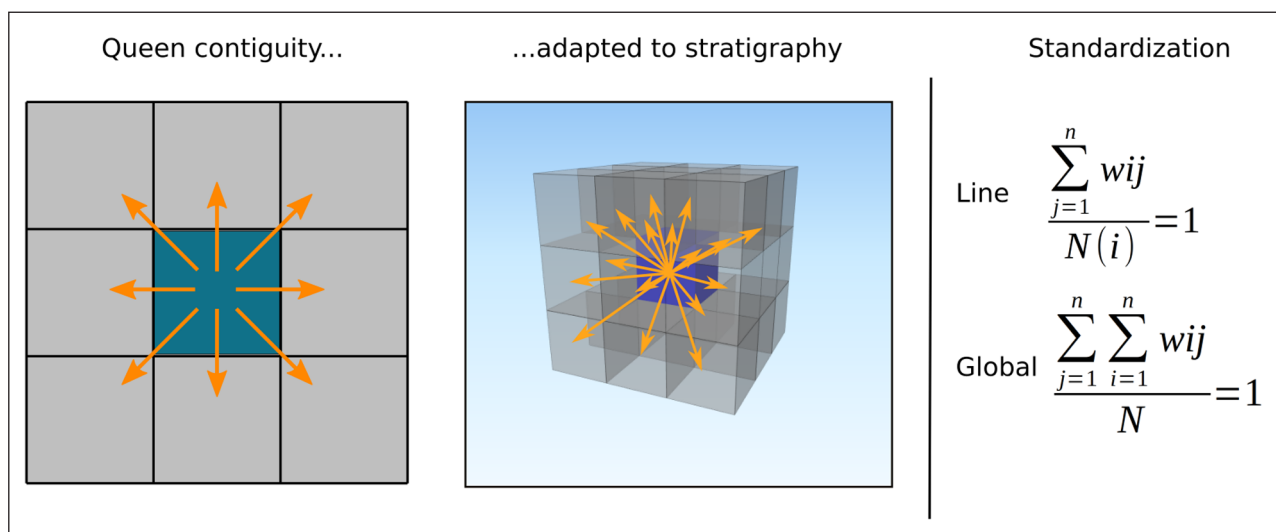


**Figure 7** Illustration of the construction of a contiguity matrix and of the two standardization methods used to produce spatial weight matrices applied to the computation of spatial analysis indices.

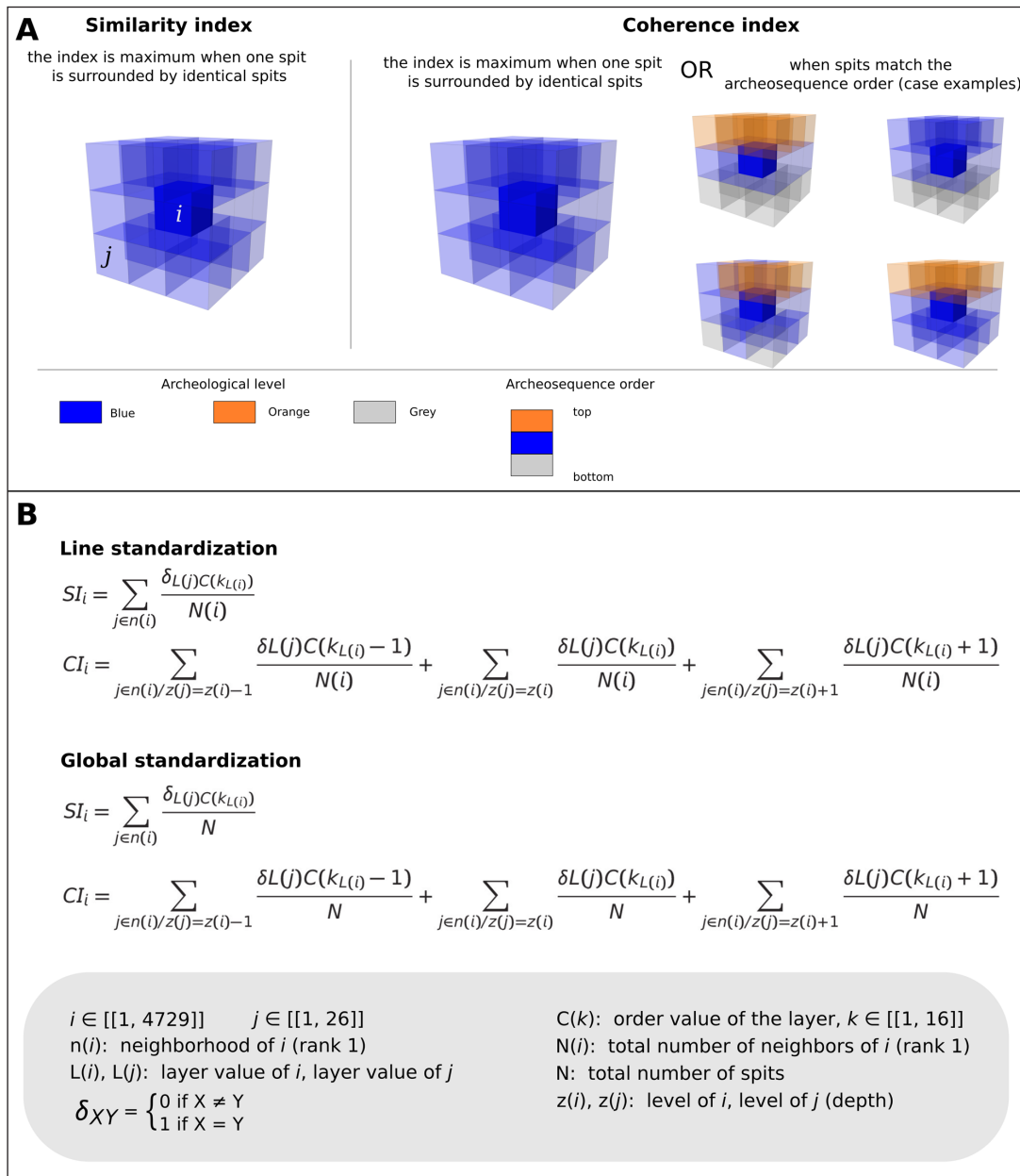


**Figure 8** Methods used to define the similarity index (SI) and coherence index (CI). A: graphical representation using theoretical data; B: mathematical formulas.

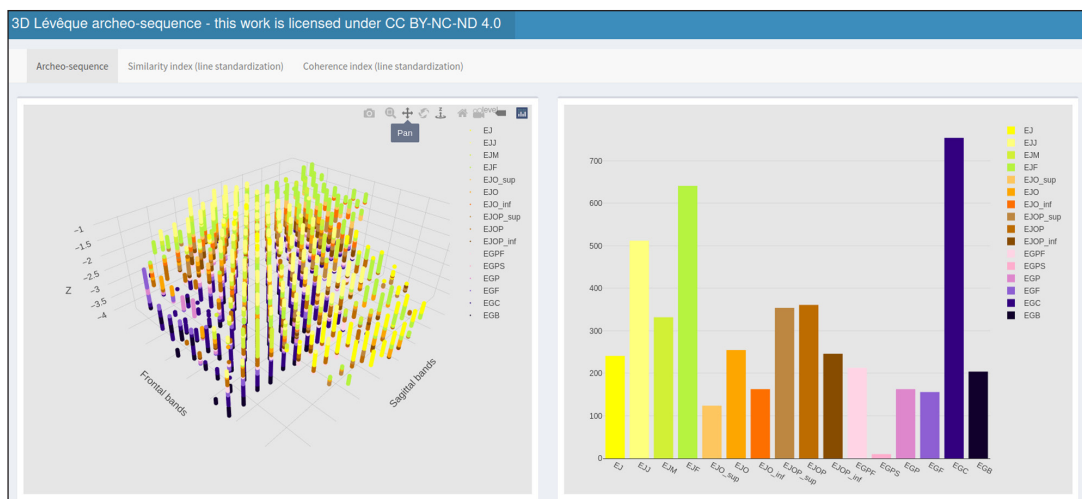


**Figure 9** First window of the visualization application with the 3D reconstruction of Lévêque's archeological sequence (left) and the number of spits per stratigraphic level (right).



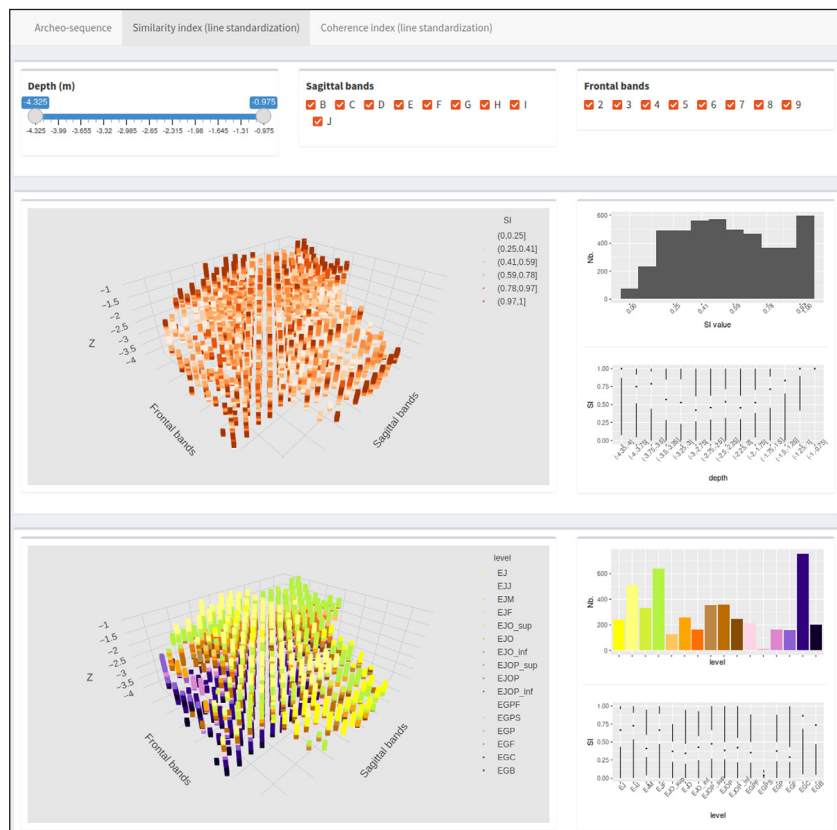


**Figure 10** Second window of the visualization application, part one (example of the similarity index [SI] computed with the line standardization method). Top: choice of dimension values; middle: 3D visualization of index values (left) and distribution charts of the spit numbers by index value and of the index values by depth for the selected spits (right); bottom: 3D visualization of stratigraphic levels (left) and distribution charts of the spit numbers by level and of the index values by level for the selected spits (right).

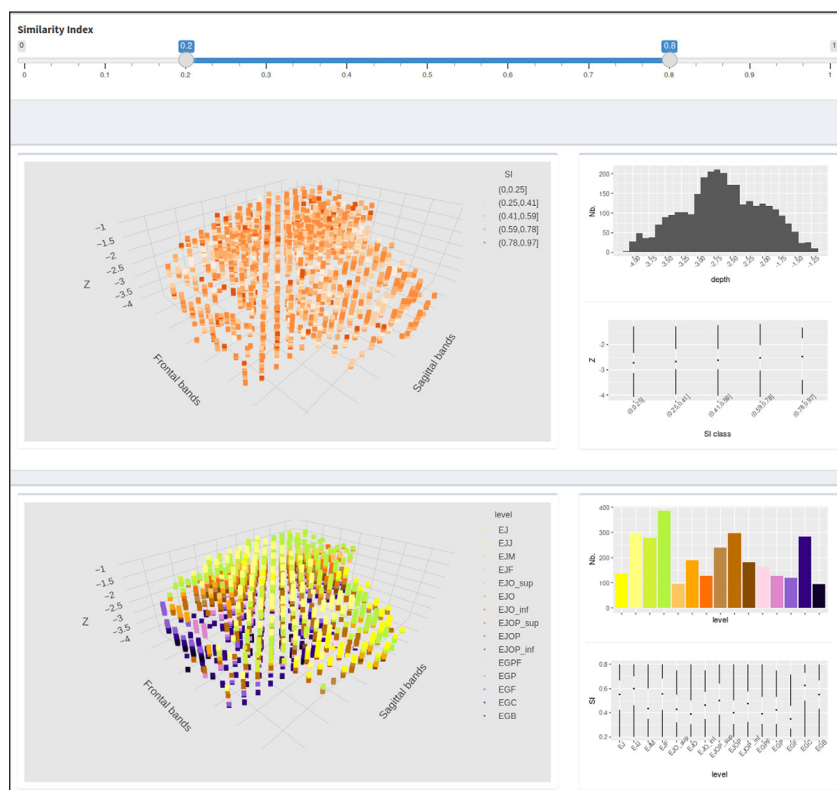


**Figure 11** Second window of the visualization application, part two (example of the similarity index [SI] computed with the line standardization method). Top: choice of index values; middle: 3D visualization of index values (left) and distribution charts of the spit numbers by depth and of the depths by index value for the selected spits (right); bottom: 3D visualization of levels (left) and distribution charts of the spit numbers by level and of the index values by level for the selected spits (right).

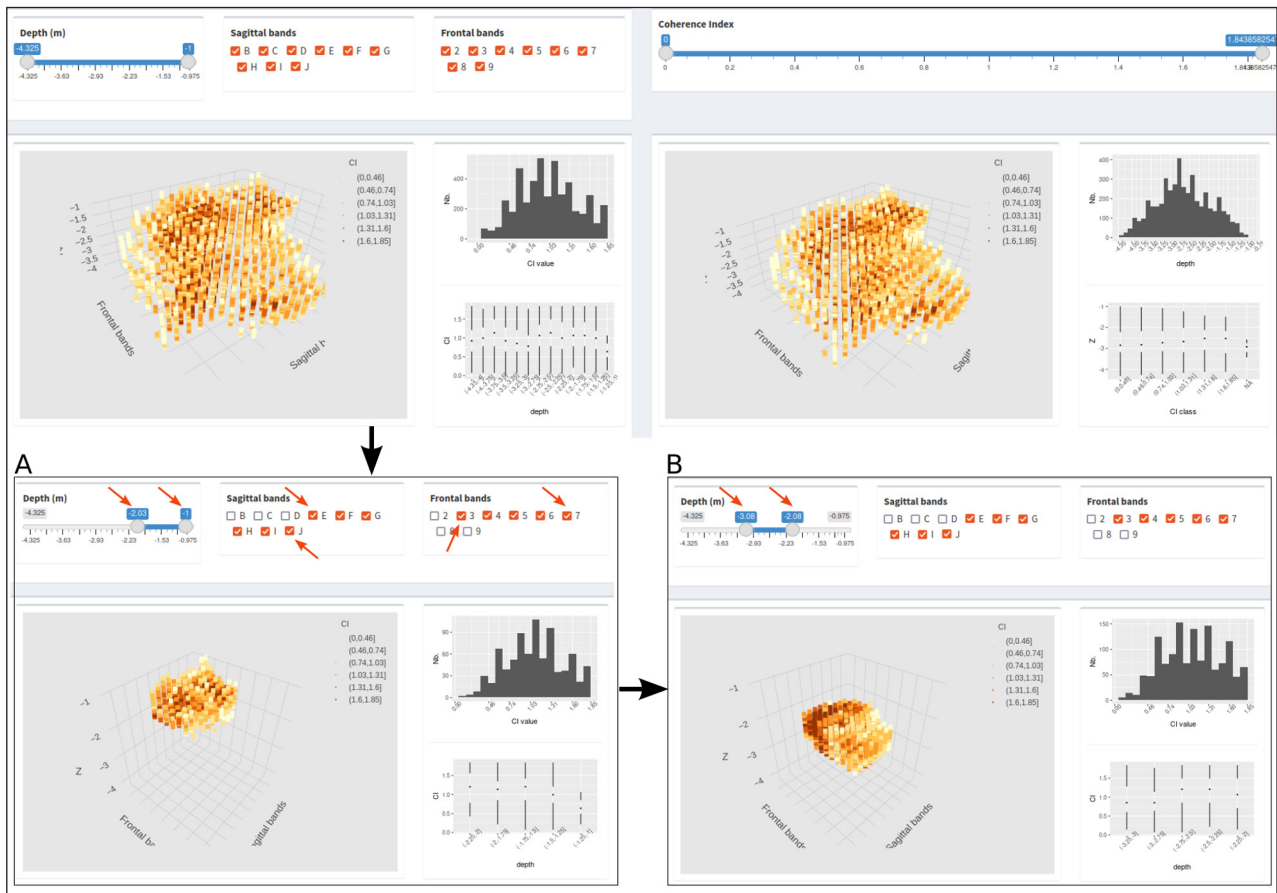


**Figure 12** Window of visualization of the coherence index. Top: overview of the indices of the whole site with every option selected; bottom left: selection of the representation of the coherence indices by spit based on specific depths, sagittal and frontal bands (red arrows); bottom right: same grid selection as on the bottom left, but with a different depth selection (red arrows).

### 3.2 SIMILARITY INDEX AND COHERENCE INDEX CHART DISTRIBUTION

To gain a better understanding of how the indices vary within the archeological site, charts were produced according to the three spatial dimensions (one chart per dimension; *Figures 13* and *14*). For each of them (sagittal bands, frontal bands, and depth levels), four different parameters are represented: 1) the index distribution (whose shape is modelled after the method of Tufte 2001), 2) the average number of spits in bands and depth levels that are taken into account to calculate indices, 3) the index average for the whole site, and 4) the location of the Saint-Césaire 1 remains.

As expected (cf. 2.3), we observe a correlation between the index values (SI and CI) and the average number of cells (spits) taken into account to calculate them, which is particularly visible at the edges of the site (*Figures 13* and *14*). With matrix construction by line standardization, there is an inverse correlation, whereas the correlation is positive for global standardization. Interpretation of the index values will therefore be valid only for spits located in a sufficiently central position, as is the case for the area that yielded the Saint-Césaire 1 remains, for instance.

For line standardization, it is worth noting that the average of the similarity indices was lower than that of the coherence indices (0.56 and 0.73, respectively), which seems consistent insofar as the calculation methods allow a greater likelihood of one of the neighbors of the considered spit having a value of 1 when computing the neighborhood matrix of the CI than of the SI (*Figure 8*).

In the value distribution chart by sagittal band (from east to west), the indices appear to be very homogeneous and always quite close to the average for the deposit as a whole. Additionally, the edge effect is very prominent with line standardization.

As far as the distance from the cliff is concerned, a decrease in index values was identified starting from sagittal bands 5/6. Importantly, the slope break observed previously on the overall visualization of the deposits lies precisely in these bands (with Saint-Césaire 1 being located in band 4).

Regarding the depth chart, it is apparent that there is a drop in the indices from a depth of -1.6 m downwards, with a concentration of low values between -2.0 and -3.0 m for the similarity indices, and an additional substantial drop between -2.5 and -3.0 m for the coherence indices.

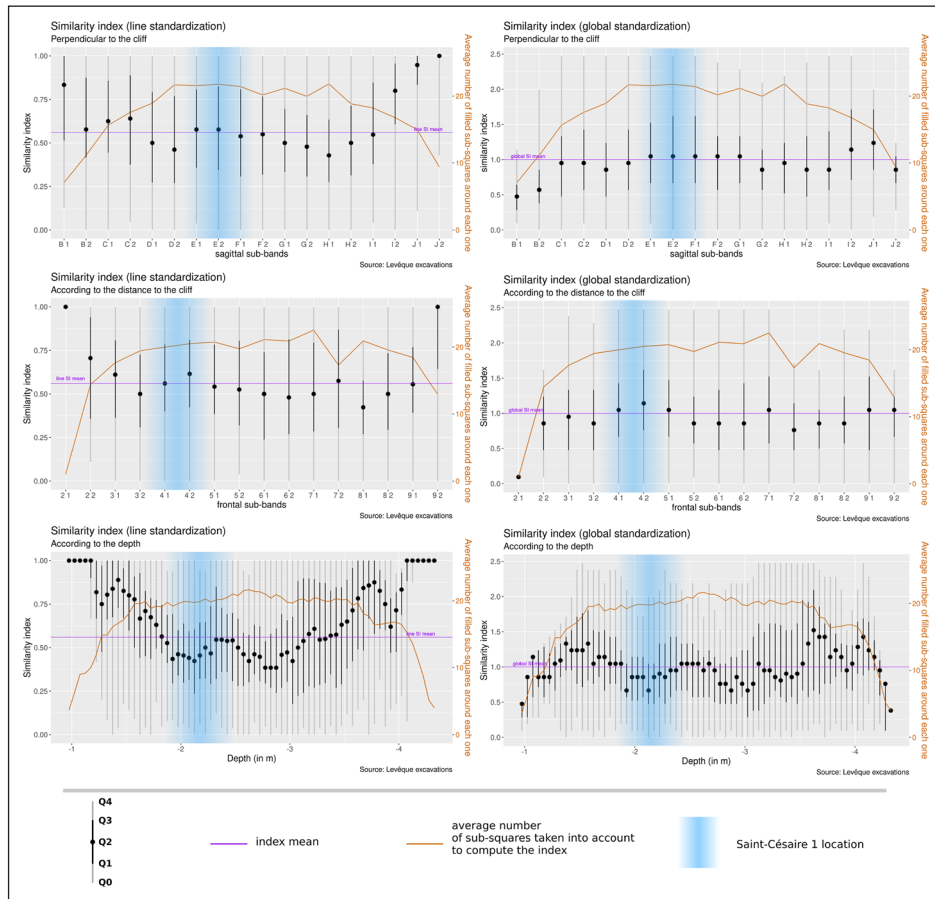


**Figure 13** Distribution of the similarity index values computed using the line (left) and global (right) standardization methods according to different dimensions (top: sagittal band; middle: frontal band; bottom: depth level).

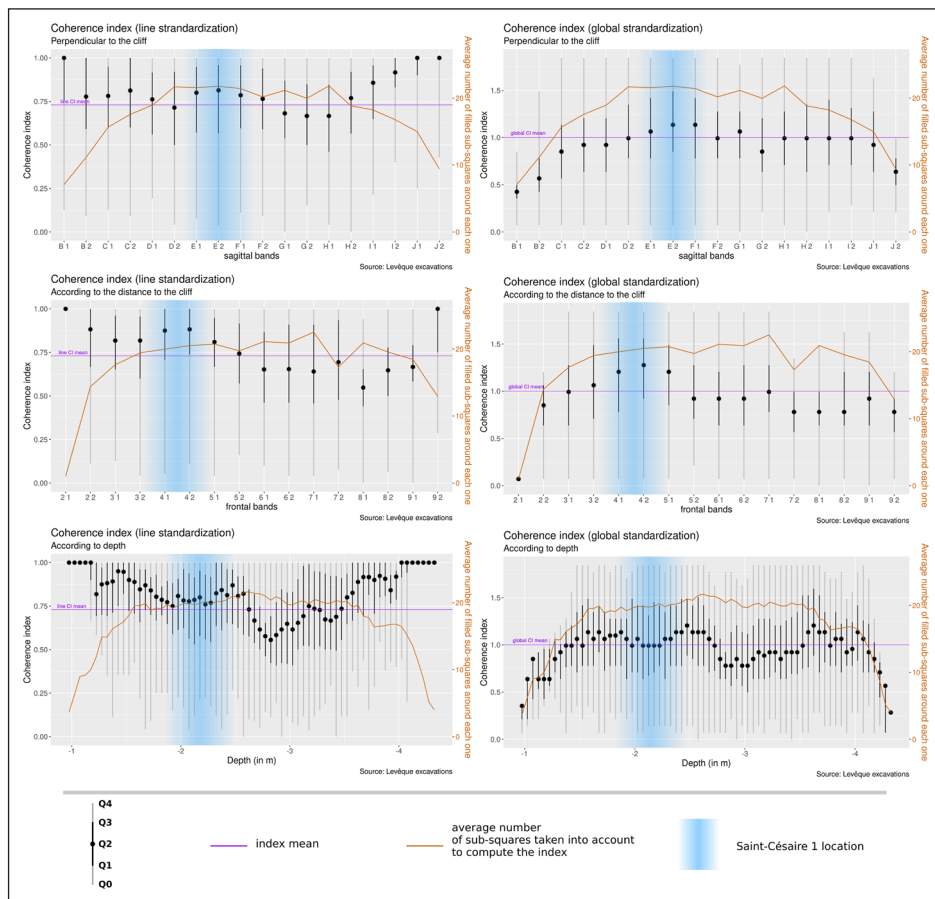


**Figure 14** Distribution of the coherence index values computed using the line (left) and global (right) standardization methods according to different dimensions (top: sagittal band; middle: frontal band; bottom: depth level).

## 4 DISCUSSION

Geovisualization tools and 3D spatial statistics offer new analytical perspectives in providing useful information about the geometry of deposits and their coherence. In cases where inconsistencies are observed, the use of appropriate indices, such as the similarity and coherence indices, allows taphonomical inferences to be made and any bias potentially related to the topography, spatial heterogeneity of the deposits, excavation history, or primary data acquisition/recording to be discussed.

### 4.1 COMPLEMENTARITY OF THE INDICES AND OF THE NEIGHBORHOOD MATRIX STANDARDIZATION MODE

The two calculated indices, SI and CI, provide complementary elements for understanding the structure of the site. The similarity index informs strictly of the resemblance between each sub-square and its neighborhood, while the coherence index can test this resemblance with respect to a pre-established spatial organization (here, the archeological sequence). While interpretation of the SI is easy for high or very low values, it becomes more subtle for intermediate values, and the complementarity of the CI then takes on its full meaning. For instance, a sub-square with a rather low SI value may be located in a coherent position with regard to the archeological sequence, which will be revealed by a rather high CI value (Figures 13 and 14). Only an expert eye can then suggest a plausible interpretation.

The neighborhood matrix standardization modes used here are also complementary. While line standardization gives more weight to observations located at the edge

of the study area (therefore with a small number of neighbors), for global standardization, on the contrary, the observations located in the center of the study area, with a large number of neighbors, are subject to more external influences than the peripheral areas. In our case, this implies that line standardization produces high index values at the edges of the site and that the values become lower with global standardization. However, such differences in value do not imply an opposite interpretation, but rather a complementary one: with line standardization, high index values clearly indicate either a strong similarity or a strong coherence, which must be mitigated by the low values obtained with a global standardization.

Combination of the two indices and two modes of standardization therefore allows a more refined and moderate interpretation of site organization.

### 4.2 TOPOGRAPHIC EFFECT ON INDEX VALUES

As outlined above, the method for constructing the neighborhood matrix (line vs global standardization) influences index computation results. We can then assume that the topography of the site (convex/concave profile) will likely have an influence, in particular on the edge effect. The theoretical example on which we rely here (Figure 15) and which reproduces the shape of the site (convex-concave profile) in a generalized way but only in 2D, shows that for a given depth or band, the number of cells used to calculate the indices varies according to the topography and arbitrary shape of the spits. In the case of a break of slope, the number of cells used to calculate the index of a given spit is rather low and the average number of spits taken into account drops, as illustrated

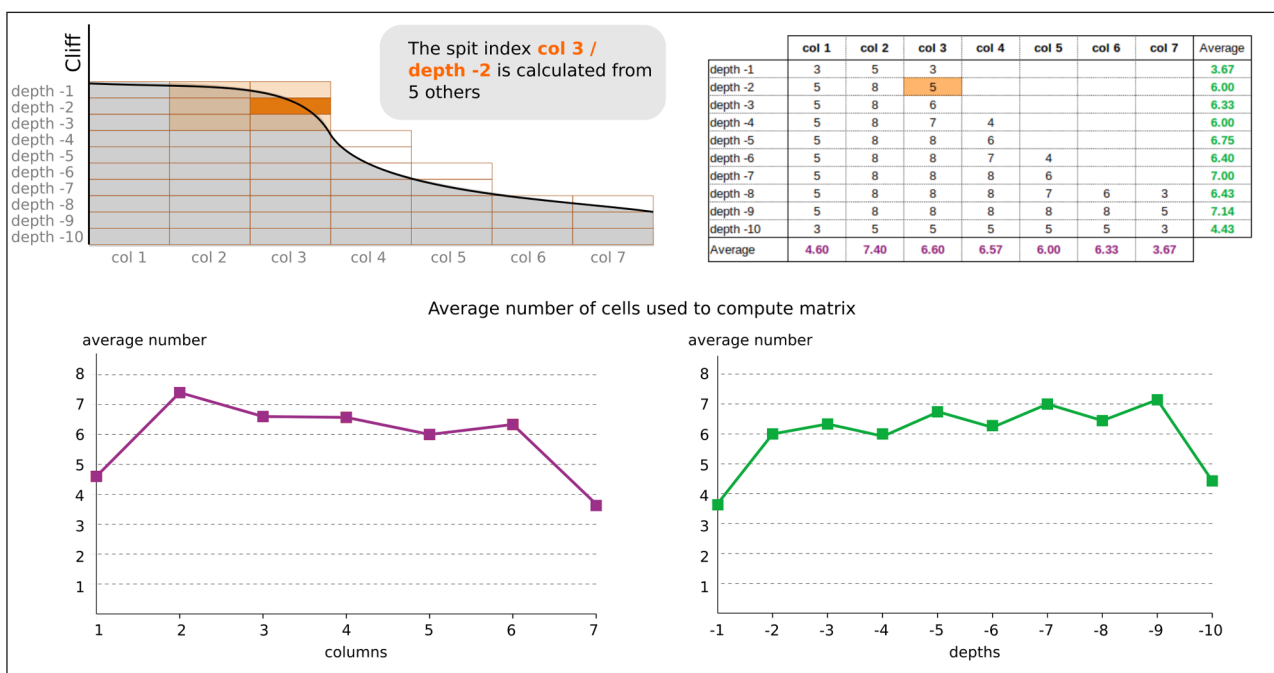


Figure 15 Influence of site topography on the average number of cells used to compute the index matrices (theoretical data).

by the theoretical example on [Figure 15](#). Such patterns can be observed at La Roche-à-Pierrot ([Figures 13 and 14](#)).

In addition, the various excavation seasons have revealed the presence of limestone blocks in the lithosequence, which are likely to generate empty spaces (no spits). Around the edges of these voids, the number of spits taken into account decreases again, as does their average number, thereby acting on the calculation of the index values ([Figure 16](#)). Such a pattern can be observed at La Roche-à-Pierrot in sagittal band 7 and at depths of between -3.70 and -3.85 m ([Figures 13 and 14](#)).

### 4.3 SPATIAL VARIABILITY OF SEDIMENTARY FACIES

It seems important to provide some perspective on the archeological stratigraphy drawn up by Miskovsky and Lévêque (1993) and based on a reference section located in a proximal sector (i.e the area of the site closest to the cliff), which is undoubtedly not representative of the whole site ([Figure 2](#)). One of the main problems with this reference section, based primarily on archeological, chromatic and sedimentological attributes observed over a limited spatial extent, is that it was used as an “idealized model” for the whole site without taking account of any potential hiatus, discordance or lateral change in the sedimentary facies. This spatial extrapolation issue is revealed by our geovisualization tools and 3D spatial statistics that show inconsistencies. Comparison of the reference section with the latest stratigraphic observations at La Roche-à-Pierrot, especially from the sagittal and frontal sections ([Figure 1](#)), reveals that diamictic facies from the archeological sequence may

change along the slope in terms of their matrix/clast ratio and of chromatic differences. From the middle part of the sagittal section (bands 5 and 6), direct correlations with the reference section appear tentative, which could explain why a decrease in the coherence indices is observed as the distance from the adjacent cliff increases ([Figure 17A](#)). This difficulty is due in particular to the fact that any stratigraphic correspondence and distal correlation must integrate the spatial variability of the lithofacies in connection with the distance from the cliff.

In addition to the matrix chromatic distinction between the yellow and gray sequences, there are probably differences in terms of fine-grained sediment inputs and varying degrees of admixture between allochthonous (sandy clay/clayey sand) and autochthonous (carbonated silty sands/sands or limestone blocks) sedimentary sources along the slope. Macroscopically, the chromatic differences in the matrix of the deposits and in lithofacies composition could therefore be associated with the spatial variability of the proportions of each of the sedimentary sources.

It is also necessary to take into account the 3D geometry of the lithofacies, whose characteristics vary spatially, not only in color but also in texture and structure, depending on the depositional processes (such as mass movement, debris fall, runoff) and post-depositional factors (e.g. bioturbation) that could be involved in site formation. A residual slope currently exists in the distal part of the deposits. Although locally anthropoturbated by historical human activities, it testifies to a gradual Pleistocene sedimentary accretion that took place on a weathered limestone substratum.

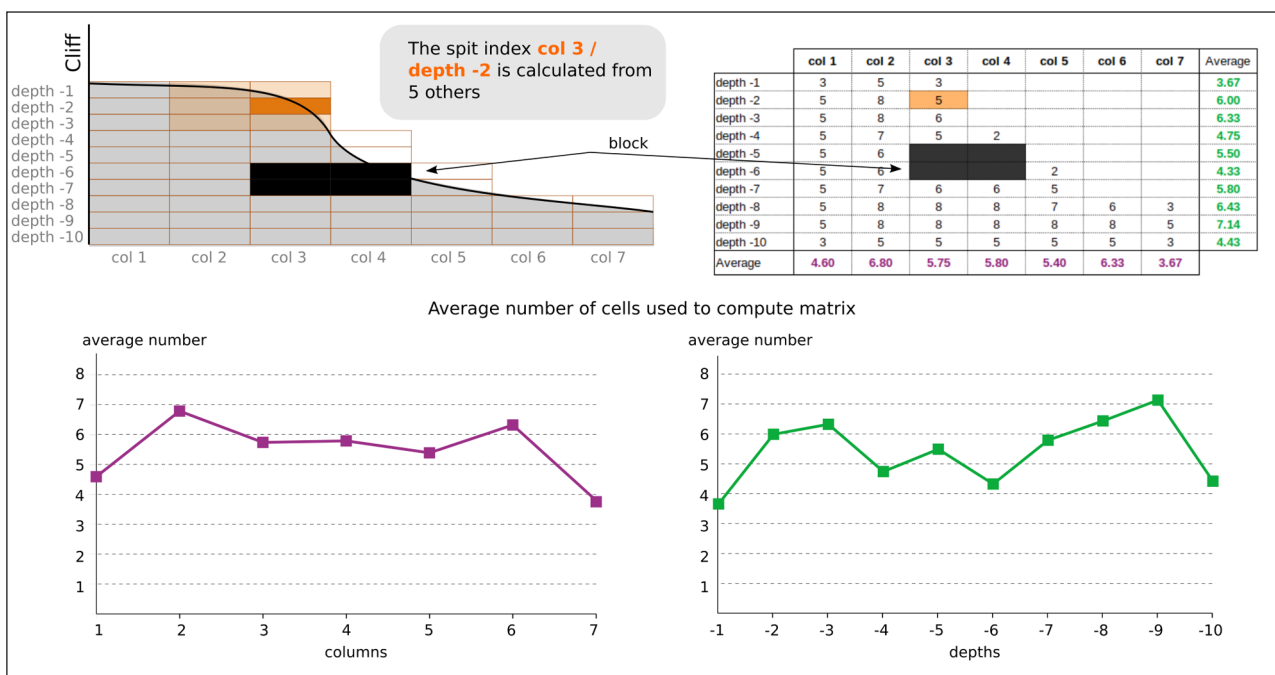


**Figure 16** Influence of site topography and the presence of blocks on the average number of cells used to compute the index matrices (theoretical data).

The topography of the latter may have influenced the final geometry of the deposits, and thereby contributed to the spatial variability of the depths from which finds that were initially assigned to the same archeological level originated.

All these elements may explain, at least in part, the spatial variability of both the similarity and coherence indices, and why defining spatially-coherent levels from the proximal to distal parts of the site is difficult when using Lévêque’s reference section. Lévêque (1997, p. 283, our translation) himself underlined the spatial variability of the stratigraphy: “...in other sectors of the deposit, the recorded stratigraphies are sometimes less complete. We can see that the Mousterian, Castelperronian and Aurignacian present three different dips. Indeed the subhorizontal Mousterian levels for about ten meters from the cliff then mark a significant dip thereafter; the three levels of Mousterian with denticulates which were quite distinct no longer form a single layer. From the bottom of the shelter, the Castelperronian presents a slight inclination. On the other hand, the Aurignacian levels are characterized by a strong dip; very thick towards the bottom of the shelter, their thickness decreases rapidly after a few meters.” In her spatial analysis of the EJOP level, Backer (1993, p. 105) also underlined the difficulties in interpreting the squares in the distal zone stratigraphically: “The windward squares G8, G9, E9, and H7 were also omitted because of difficulties with stratigraphic interpretation in the field: The Castelperronien level was indistinguishable from Aurignacian deposits in these squares and thus was lumped with them.”

#### 4.4 ANTHROPOGENIC BIAS

Identification of the archeological sequence on the basis of a fixed reference section (Figures 1 and 2) close

to the cliff, without taking into account the geometry of the deposits (cf. *supra*), may have been a source of anthropogenic bias when spatially extrapolated to the whole site, even by trained archeologists. In addition, the Lévêque excavations were organized in a checkerboard pattern, with some squares remaining dormant for several years. Finally, the volunteer excavators were not necessarily trained in stratigraphic reading, which could lead to recording errors. Certain passages from the excavation notebooks illustrate this issue through the testimony of the excavators on their difficulties identifying certain levels (e.g. square H5 notebook, entry of 11/07/1981 that explains a correction from EJM to EJF for sub-square H5 III, spit 176–190 [our translation]: “Problem: !! According to the latest information, we should be in EJF [...]: the layer of flint present in secondary squares I, II and IV and absent in III would appear to correspond to EJM. We should also note a difference in compactness between EJM (very loose) and EJF, the bone layer (much more compact). However, the color is similar. The next labels will bear the name EJF”). These observations help to explain the variations in indices observed across the site.

In addition to these problems inherent in the excavation, the archives of F. Lévêque and A. Backer report anthropoturbations of the deposits (Backer 1994). Some of these disturbances may be linked to medieval occupation or to the exploitation of the quarry which led to the discovery of the site, while others appear to be the result of clandestine excavations. Figure 17B shows the location of such disturbances of mechanical and clandestine origins in the upper levels of the F-G-H bands, near the rock face. These zones are correlated with a decrease in the density of the high values of coherence indices in an otherwise well-preserved area of the site (Figure 17A).

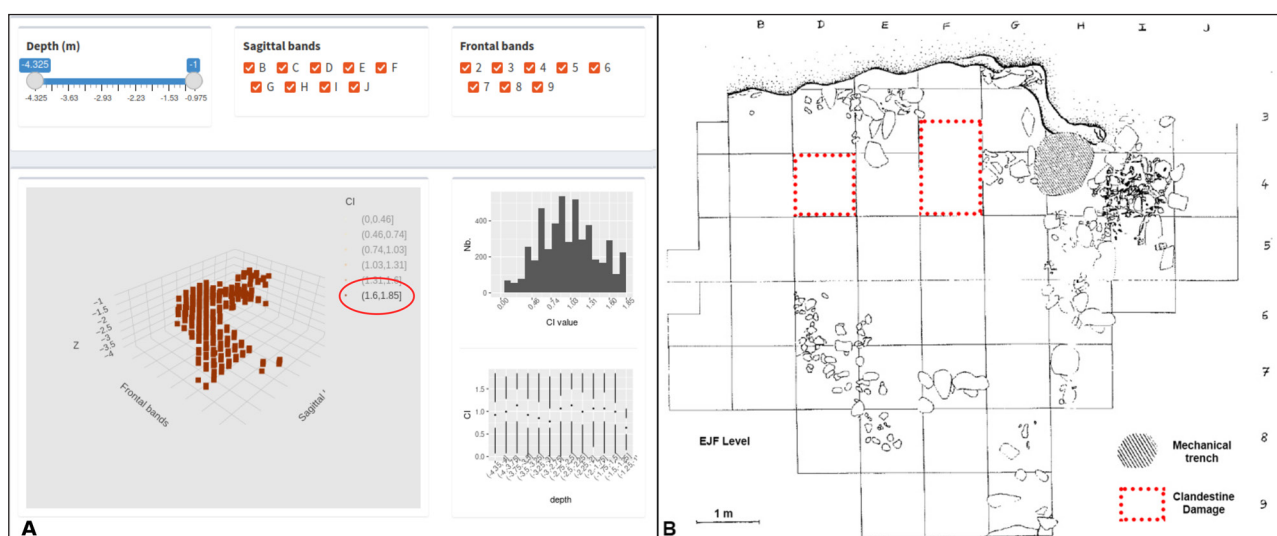


**Figure 17** Visualization of the highest range of coherence indices of La Roche-à-Pierrot (left) and map of the site area excavated by F. Lévêque with location of the sectors with mechanical and clandestine excavation disturbances in level EJF (right; modified from Backer 1994).

## 5 CONCLUSION

The tools developed in this research provide a new descriptive and analytical approach for investigating archeological data retrieved from archives by 3D georeferenced visualization of primary recordings and also by computing spatial statistics using the Queen contiguity of the archeological sequence. Computation of both the similarity and coherence indices allows the geometry of the deposits and spatial inconsistencies to be outlined and then discussed in light of the original archeostratigraphic model of the site, as illustrated here with La Roche-à-Pierrot.

The descriptive and analytical possibilities offered by the new approach are not limited to use with spit data, but will allow other sources of archival data to be integrated, such as piece-plotted elements. In addition, the new tool presented here can be combined with the development of a virtual application at La Roche-à-Pierrot (VRPB; Lacrampe-Cuyaubère et al. 2021) that includes all of the digital data produced by the new excavations at the site (e.g. 3D photogrammetric-recorded models of every spit, georeferencing of samples and piece-plotted elements, and surface models of significant elements). Ultimately, the combination of these different approaches will allow us to generate an integrated model of all of the data produced during the original and ongoing excavations at La Roche-à-Pierrot.

The digital workflow and related tools presented here for visualizing and analyzing the stratigraphic attributes and geospatial information at La Roche-à-Pierrot will certainly be useful for other archeological projects where excavation archives and/or archeological stratigraphy data are available. The present methodology highlights novel avenues for future research, such as the design of applications and analytical tools that could assist in expanding analyses by incorporating the computation of the spatial autocorrelation (Anselin 1988). The latter is well suited to categorical data (Boots 2003) and enables the location and identification of places in the structure where spits appear similar and places where they do not. The development of 3D spatial autocorrelation indices by adapting the global or local Moran to the Queen contiguity of the archeological sequence will give us information about statistically significant locations, especially at microlocal scale (i.e. spatial clusters).

Although geovisualization tools and 3D spatial statistics may present some practical and specific technical limitations, they also provide valuable information for discussing site formation processes, whether anthropogenic or natural. Ultimately, these new tools will allow us to reassess and enhance primary information from old excavations that may not have been conducted to today's standards. More specifically, they will revive the legacy of past excavations and

increase the importance of formerly excavated sites in the archeological record.

## ACKNOWLEDGEMENTS

We are thankful to C. Schwab, curator of the Paleolithic and Mesolithic collections of the Musée d'Archéologie nationale (MAN, Saint-Germain-en-Laye, France), for granting us access to the Saint-Césaire faunal collection. We are grateful to C. Jouys-Barbelin and S. Morinière from the Resource center of the MAN, in charge of the curation of F. Lévêque's archives, for their help and support in accessing the original excavation notebooks. We also thank E. Morin (Trent University) for sharing information with us about F. Lévêque's excavations. HR received funding from the CSUN Competition for Research, Scholarship and Creative Activity Awards and from several research-supporting programs of the College of Social and Behavioral Sciences of CSUN (Research Competition, Summer Research Stipend, and Research Fellowship). The Collective Research Project of La Roche-à-Pierrot is funded by the Direction régionale des affaires culturelles of the Nouvelle-Aquitaine Region and by the Charente-Maritime Department, France. Finally, we thank the TGIR Huma-Num team (<https://www.huma-num.fr/>) for their technical support and R. Lemoy (Rouen Normandie University, CNRS UMR 6266 IDEES) for his help with formatting of the index formulas.

## COMPETING INTERESTS

The authors have no competing interests to declare.

## AUTHOR AFFILIATIONS

**Armelle Couillet**  [orcid.org/0000-0002-2285-0263](https://orcid.org/0000-0002-2285-0263)

Rouen Normandie University, CNRS UMR 6266 IDEES, 76130 Rouen, FR

**Hélène Rougier**  [orcid.org/0000-0003-0358-0285](https://orcid.org/0000-0003-0358-0285)

Department of Anthropology, California State University Northridge, Northridge, CA 91330-8244, US; Max Planck Institute for Evolutionary Anthropology, 04103 Leipzig, DE

**Dominique Todisco**  [orcid.org/0000-0001-7929-0204](https://orcid.org/0000-0001-7929-0204)

Rouen Normandie University, CNRS UMR 6266 IDEES, 76130 Rouen, FR

**Josserand Marot**

Service Départemental d'Archéologie de Charente-Maritime, 17100 Saintes, FR

**Olivier Gillet**  [orcid.org/0000-0001-7541-8282](https://orcid.org/0000-0001-7541-8282)

Rouen Normandie University, CNRS UMR 6266 IDEES, 76130 Rouen, FR

**Isabelle Crevecoeur**  [orcid.org/0000-0002-1781-3206](https://orcid.org/0000-0002-1781-3206)

UMR 5199 PACEA, CNRS, Université de Bordeaux, 33615 Pessac, FR

## REFERENCES

- Anselin, L. 1988. *Spatial Econometrics: Methods and Models*. Dordrecht: Kluwer Academic. DOI: <https://doi.org/10.1007/978-94-015-7799-1>
- Anselin, L. 2020. *Contiguity-based spatial weights*. Available at [http://ghhttp://geodacenter.github.io/workbook/4a\\_contig\\_weights/lab4a.html](http://ghhttp://geodacenter.github.io/workbook/4a_contig_weights/lab4a.html) [Last accessed 5 Mai 2021]
- Bachelier, F, Caux, S, Crevecoeur, I, Gravina, B, Mallol, C, Maureille, B, Michel, A, Rougier, H, Tartar, E, Teyssandier, N, Bordes, JG and Morin, E. 2014. Preliminary results from ongoing excavations at La Roche à Pierrot, Saint-Césaire. Poster presented at the XVII World UISPP Congress, Burgos (Spain), 1–7 September 2014.
- Backer, A. 1994. *Site Structure of Saint-Césaire: Changing Uses of a Paleolithic Rockshelter*. Unpublished thesis (PhD), Albuquerque: University of New Mexico.
- Backer, A. 1997. *Rapport sur le Sauvetage Urgent de 1997, Saint-Césaire (Charente-Maritime). Rapport de fouilles programmées*. DRAC Poitou-Charentes, SRA.
- Backer, AM. 1993. Spatial distributions at La Roche-à-Pierrot, Saint-Césaire: changing uses of a rockshelter. In: Lévêque, F, Backer, AM and Guilbaud, M (eds.), *Context of a Late Neandertal. Implications of Multidisciplinary Research for the Transition to Upper Paleolithic Adaptations at Saint-Césaire, Charente-Maritime, France*, 105–127. Madison: Prehistory Press.
- Bar-Yosef, O and Bordes, JG. 2010. Who were the makers of the Châtelperronian culture? *Journal of Human Evolution*, 59(5): 586–593. DOI: <https://doi.org/10.1016/j.jhevol.2010.06.009>
- Bertin, J. 1967. *Sémiologie graphique. Les diagrammes, les réseaux, les cartes*. Paris-La Haye: Mouton and Co Paris Gauthier-Villars.
- Bivand, RS, Pebesma, EJ and Gómez-Rubio, V. 2008. *Applied Spatial Data Analysis with R*. New York: Springer-Verlag.
- Boots, B. 2003. Developing local measures of spatial association for categorical data. *Journal of Geographical Systems*, 5(2): 139–160. DOI: <https://doi.org/10.1007/s10109-003-0110-3>
- Brath, R. 2014. 3D InfoVis is here to stay: Deal with it. In: 2014 *IEEE VIS International Workshop on 3DVis (3DVis)*, 25–31. DOI: <https://doi.org/10.1109/3DVis.2014.7160096>
- Crevecoeur, I. 2017. Reprise des fouilles à la Roche-à-Pierrot, Saint-Césaire. In: Cleyet-Merle, JJ, et al. (eds.), *Le troisième Homme. Préhistoire de l'Altai*, 107. Paris: Editions de la Réunion des musées nationaux.
- Dilena, MA and Soressi, M. 2020. Reconstructive archaeology: In situ visualisation of previously excavated finds and features through an ongoing mixed reality process. *Applied Sciences*, 10(21): 7803. DOI: <https://doi.org/10.3390/app10217803>
- Discamps, E, Bachelier, F, Baillet, M and Sitzia, L. 2019. The use of spatial taphonomy for interpreting pleistocene palimpsests: An interdisciplinary approach to the Châtelperronian and carnivore occupations at Cassenade (Dordogne, France). *PaleoAnthropology*, 2019: 362–388.
- Discamps, E, Muth, X, Gravina, B, Lacrampe-Cuyaubère, F, Chadelle, JP, Faivre, JP and Maureille, B. 2016. Photogrammetry as a tool for integrating archival data in archaeological fieldwork: Examples from the Middle Palaeolithic sites of Combe-Grenal, Le Moustier, and Regourdou. *Journal of Archaeological Science: Reports*, 8: 268–276. DOI: <https://doi.org/10.1016/j.jasrep.2016.06.004>
- Galeazzi, F. 2015. Towards the definition of best 3D practices in archaeology: Assessing 3D documentation techniques for intra-site data recording. *Journal of Cultural Heritage*, 17: 159–169. DOI: <https://doi.org/10.1016/j.culher.2015.07.005>
- Galeazzi, F, Callieri, M, Dellepiane, M, Charno, M, Richards, J and Scopigno, R. 2016. Web-based visualization for 3D data in archaeology: The ADS 3D viewer. *Journal of Archaeological Science: Reports*, 9: 1–11. DOI: <https://doi.org/10.1016/j.jasrep.2016.06.045>
- Gravina, B, Bachelier, F, Caux, S, Discamps, E, Faivre, JP, Galland, A, Michel, A, Teyssandier, N and Bordes, JG. 2018. No reliable evidence for a Neanderthal-Châtelperronian association at La Roche-à-Pierrot, Saint-Césaire. *Scientific Reports*, 8: 15134. DOI: <https://doi.org/10.1038/s41598-018-33084-9>
- Hietala, H. (ed.) 1984. *Intrasite spatial analysis in archaeology (New directions in archaeology)*. Cambridge: Cambridge University Press.
- Hodder, I and Orton, C. 1976. *Spatial analysis in archaeology. New studies in archaeology*, 1. New York & London: Cambridge University Press.
- Kraus, M, Fuchs, J, Sommer, B, Klein, K, Engelke, U, Keim, D and Schreiber, F. 2021. Immersive analytics with abstract 3D visualizations: A survey. *Computer Graphics Forum*. DOI: <https://doi.org/10.1111/cgf.14430>
- Lacrampe-Cuyaubère, F, Beauval, C, Marot, J, Crevecoeur, I and Rougier, H. 2021. Suivi microtopographique des fouilles de La Roche-à-Pierrot et développements de l'application VRPB. Note sur l'avancée des travaux en 2020. In: Crevecoeur, I (resp.), *La Roche-à-Pierrot (Saint-Césaire, Charente-Maritime), Rapport du PCR et de la fouille programmée 2020*, 83–98. Report submitted to the Service Régional de l'Archéologie de Nouvelle-Aquitaine, France.
- Lercari, N. 2017. 3D visualization and reflexive archaeology: A virtual reconstruction of Çatalhöyük history houses. *Digital Applications in Archaeology and Cultural Heritage*, 6: 10–17. DOI: <https://doi.org/10.1016/j.daach.2017.03.001>
- Lévêque, F. 1997. Le Passage du Paléolithique moyen au Paléolithique supérieur: Données stratigraphiques de quelques gisements sous-grotte du sud-ouest. *Quaternaire*, 8(2–3): 279–287. DOI: <https://doi.org/10.3406/quate.1997.1580>
- Lévêque, F. 2002. Méthodes de fouilles. In: Miskovsky, JC (ed.), *Géologie de la préhistoire: Méthodes, techniques, applications*, 415–423. Paris: GéoPré.
- Lévêque, F, Backer, AM and Guilbaud, M. 1993. *Context of a Late Neandertal. Implications of Multidisciplinary Research for the*



- Transition to Upper Paleolithic Adaptations at Saint-Césaire, Charente-Maritime, France*. Madison: Prehistory Press.
- Lévêque, F** and **Vandermeersch, B**. 1980. Découverte de restes humains dans un niveau castelperronien à Saint-Césaire (Charente-Maritime). *Comptes Rendus de l'Académie des Sciences de Paris*, 291: 187–189.
- Lévêque, F** and **Vandermeersch, B**. 1981. Nouvelles. *Bulletins et Mémoires de la Société d'Anthropologie de Paris*, 8: 103–104. DOI: <https://doi.org/10.3406/bmsap.1981.3812>
- Mellars, P**. 2004. Neanderthals and the modern human colonization of Europe. *Nature*, 432: 461–465. DOI: <https://doi.org/10.1038/nature03103>
- Minoru, A**. 2013. *Qgis2threejs*, Version 2.6. Available at <https://github.com/minorua/Qgis2threejs> [Last accessed 5 Mai 2021]
- Miskovsky, JC** and **Lévêque, F**. 1993. The sediments and stratigraphy of Saint-Césaire: Contributions to the paleoclimatology of the site. In: Lévêque, F, Backer, AM and Guilbaud, M (eds.), *Context of a Late Neandertal. Implications of Multidisciplinary Research for the Transition to Upper Paleolithic Adaptations at Saint-Césaire, Charente-Maritime, France*, 9–14. Madison: Prehistory Press.
- Oppenhaffen, L**. 2021. Visualizing archaeologists: A reflexive history of visualization practice in Archaeology. *Open Archaeology*, 7(1): 353–377. DOI: <https://doi.org/10.1515/oper-2020-0138>
- Talamo, S, Aldeias, V, Goldberg, P, Chiotti, L, Dibble, HL, Guérin, G, Hublin, JJ, Madelaine, S, Maria, R, Sandgathe, D, Steele, TE, Turq, A** and **Mcperron, SJP**. 2020. The new <sup>14</sup>C chronology for the Palaeolithic site of La Ferrassie, France: the disappearance of Neanderthals and the arrival of *Homo sapiens* in France. *Journal of Quaternary Science*, 35: 961–973. DOI: <https://doi.org/10.1002/jqs.3236>
- Tiefelsdorf, M**. 1998. *Modelling spatial processes: The identification and analysis of spatial relationships in regression residuals by means of Moran's I (Germany)*. Unpublished thesis (PhD), Canada: Wilfrid Laurier University.
- Tufte, ER**. 2001. *The visual display of quantitative information (second edition)*. Cheshire: Graphics Press.
- Van Wijk, JJ**. 2005. The value of visualization. In: *VIS 05. IEEE Visualization, 2005*, 79–86. DOI: <https://doi.org/10.1109/VISUAL.2005.1532781>
- Zilhão, J** and **d'Errico, F**. 1999. The chronology and taphonomy of the earliest Aurignacian and its implications for the understanding of Neandertal extinction. *Journal of World Prehistory*, 13(1): 1–68. DOI: <https://doi.org/10.1023/A:1022348410845>

---

#### TO CITE THIS ARTICLE:

Couillet, A, Rougier, H, Todisco, D, Marot, J, Gillet, O and Crevecoeur, I. 2022. New Visual Analytics Tool and Spatial Statistics to Explore Archeological Data: The Case of the Paleolithic Sequence of La Roche-à-Pierrot, Saint-Césaire, France. *Journal of Computer Applications in Archaeology*, 5(1), 19–34. DOI: <https://doi.org/10.5334/jcaa.81>

Submitted: 02 August 2021 Accepted: 21 January 2022 Published: 03 March 2022

#### COPYRIGHT:

© 2022 The Author(s). This is an open-access article distributed under the terms of the Creative Commons Attribution 4.0 International License (CC-BY 4.0), which permits unrestricted use, distribution, and reproduction in any medium, provided the original author and source are credited. See <http://creativecommons.org/licenses/by/4.0/>.

*Journal of Computer Applications in Archaeology* is a peer-reviewed open access journal published by Ubiquity Press.